Journal of Power Sources 190 (2009) 86–91

Contents lists available at ScienceDirect

Journal of Power Sources

journal homepage: www.elsevier.com/locate/jpowsour

Prevention of fuel cell starvation by model predictive control of pressure, excess ratio, and current

Michael A. Danzer*, Simon J. Wittmann, Eberhard P. Hofer

Institute of Measurement, Control and Microtechnology, Ulm University, Albert-Einstein-Allee 41, 89081 Ulm, Germany

ARTICLE INFO

Article history:
Received 12 June 2008
Received in revised form 18 December 2008
Accepted 19 December 2008
Available online 30 December 2008

Keywords:
Starvation prevention
Model predictive control
Fuel cell

ABSTRACT

Starvation of polymer electrolyte fuel cells (PEFC) takes place, especially during transients, if reactants are consumed in the fuel cell faster than they can be supplied. It is one of the main causes of aging and degeneration of fuel cells.

To prevent oxidant starvation and to allow for a dynamic operation of the fuel cell, the excess ratio of oxygen needs to be adjusted rapidly by increasing the mass flow into the cathode. This increase is limited by the inertia of the actuators. Especially at fast load changes the risk of starvation is high. This problem can be faced by limiting the dynamics of load changes or by decoupling the desired load from the effective load. This work presents a decoupled approach, where the effective fuel cell current becomes a controllable variable. Consequently, the control variables are the oxygen excess ratio, the fuel cell pressure, and the effective current. To prevent starvation the control design has to guarantee that the oxygen excess ratio does not fall beyond a minimum value. This goal is achieved by model predictive control which is an optimal control scheme that incorporates actuator limitations and state constraints in the control design.

1. Introduction

An undersupply of fuel cells leads to a depletion of reactants at the reaction surface and finally to fuel cell starvation. Fuel and oxidant starvation are one of the main causes of short life and performance degradation of fuel cells [1]. When starvation occurs a reversal of the fuel cell voltage can happen and carbon corrosion takes place [2,3]. Especially during transients, starvation can occur if reactants are consumed in the fuel cell faster than they can be supplied by the delivery system. To prevent starvation corrective actions as rate limiters and reference governors for the fuel cell current, as well as fast mass flow control need to be employed [4–6].

In the following a new model of the gas dynamics of a fuel cell system, incorporating the pipes and fittings at the inlet and the outlet, the valve and the fuel cell stack is presented. It is a nonlinear model with parameters identified at a polymer electrolyte fuel cell system. To influence the transients of the fuel cell current the desired load is decoupled from the effective load. Thereby, the fuel cell current becomes a controllable variable.

To prevent starvation three actuators – the valve, the mass flow controller, and the electrical load – are used in an integrated approach. The presented model predictive control approach is a multivariable control which incorporates the pressure control, the mass flow control, and the control of the fuel cell current in one scheme. The model predictive controller calculates optimal control inputs regarding actuator limitations and constraints of the controlled variables.

2. Model of the fuel cell system

The nonlinear model of the fuel cell system describes the dynamic behaviour of the mass flows and the pressure drops of the gas supply, the fuel cell stack, the exhaust, and the outlet valve. Furthermore, a model of the mass flow controller and a model of the electrical load are incorporated.

2.1. Gas dynamics

The model of the gas dynamics is based on the law of conservation of mass and the description of laminar and turbulent flow [7,8]. The model does not account for spatial dependencies. In analogy to electronic circuits the gas dynamics is described by an equivalent circuit of lumped laminar and turbulent flow resistances, R_{lam} and R_{turb}, as well as mass storing capacitances C [9,10].

* Corresponding author. Tel.: +49 731 5026325; fax: +49 731 5026301.
E-mail address: michael.danzer@uni-ulm.de (M.A. Danzer).
URL: http://www.uni-ulm.de/en/in/mrm.html (M.A. Danzer).

0378-7753/$ – see front matter © 2008 Elsevier B.V. All rights reserved.
doi:10.1016/j.jpowsour.2008.12.089

Nomenclature

A	system matrix
B	input matrix
C	capacity
E	tracking error
f	nonlinear function
H_p	prediction horizon
J	objective function
k	discrete time index
K_{exp}	exponential parameter of the turbulent flow resistance
K_{lam}	parameter of the laminar flow resistance
K_{turb}	linear parameter of the turbulent flow resistance
m	mass
$\mathcal{NL}$	vector or matrix of nonlinearities
p	pressure
Δp	pressure difference
Q	weighting matrix
R_{lam}	laminar flow resistance
R_{turb}	turbulent flow resistance
R	weighting matrix
t	continuous time
T	sampling time
T	temperature (with index)
u	input vector
$\Delta\hat{\boldsymbol{U}}$	vector of future changes to the input vector
v	offset vector
W	mass flow
x	state vector
y	output vector
$\hat{\boldsymbol{Y}}$	vector of predicted outputs
$\hat{\boldsymbol{Y}}_f$	free response
y_{O_2}	mass fraction of oxygen in air
λ_{O_2}	excess ratio of oxygen

Greek letters

σ	correction factor
τ	time constant

Indices

0	standard conditions
c	continuous
C	capacity
d	discrete
des	desired
eff	effective
EL	electrical load
FC	fuel cell
H_2O	water
in	inlet
max	maximum
MFC	mass flow controller
min	minimum
O_2	oxygen
out	outlet
react	reaction
ref	reference
V	valve

The static behaviour of a component is determined by a nonlinear function

$$\sigma \cdot \Delta p = \sigma \cdot R \cdot W = K_{lam} W + K_{turb} W^{K_{exp}} \quad (1)$$

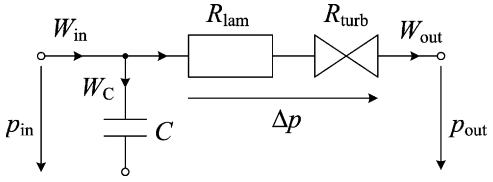

Fig. 1. Equivalent circuit of a component of the gas dynamics with laminar and turbulent flow resistance, R_{lam} and R_{turb}, and capacitance C.

of the pressure drop Δp over the component in dependence on the mass flow $W = \dot{m}$ through it, with the nonlinear flow resistance R which is composed of a laminar and a turbulent part

$$R = R_{lam} + R_{turb} = \frac{1}{\sigma} \cdot (K_{lam} + K_{turb}\ W^{K_{FC,exp}-1}). \quad (2)$$

The exponential parameter K_{exp} describes the nonlinear relation of the pressure drop and the mass flow at a turbulent flow resistance. The parameter of the laminar flow resistance K_{lam} and the parameters of the turbulent flow resistance K_{turb} and K_{exp} are constant. As a correction factor

$$\sigma = \frac{T_0 \cdot p_{in}}{T_{in} \cdot p_0} \quad (3)$$

accounts for the deviation from standard pressure and standard temperature at the inlet of the component. Therewith, the pressure difference

$$\Delta p = f(W, p_{in}, T_{in}) \quad (4)$$

is a nonlinear function of the current mass flow through the component, the temperature, and the pressure at the inlet.

The dynamic behaviour of a component is related to the capability to store mass in its volume. With the differential equation of the pressure at a capacitance C

$$\frac{d}{dt}p = \dot{p} = \frac{1}{C} \cdot W_C \quad (5)$$

and the equivalence to Kirchhoff's current law for mass flows

$$W_{in} = W_C + W \quad (6)$$

with

$$W = \frac{\Delta p}{R} = \frac{p_{in} - p_{out}}{R} \quad (7)$$

the differential equation of a component

$$W_{in} = C \cdot \dot{p}_{in} + \frac{\Delta p}{R} = C \cdot \dot{p}_{in} + \frac{p_{in} - p_{out}}{R} \quad (8)$$

results. All components as pipes, manifolds, fittings, valves, and the fuel cell stack itself can be described by equation (8) and the according equivalent circuit depicted in Fig. 1. For pipes, manifolds, and fittings the parameter K_{exp} is equal to 2. For valves, where the flow is purely turbulent, the parameter $K_{lam} = 0$ disappears.

Fig. 2 shows the whole system of the gas dynamics of a fuel cell.

All components in between the mass flow controller (MFC) and the fuel cell stack, as well as all components in between the fuel cell stack and the outlet valve are combined to one component for the inlet and one for the outlet.

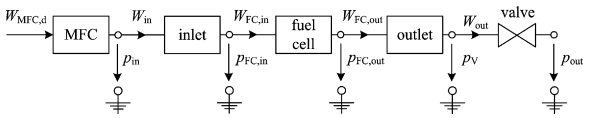

Fig. 2. Equivalent circuit of the fuel cell system comprising a mass flow controller (MFC), the fuel cell stack, inlet and outlet, and a valve.

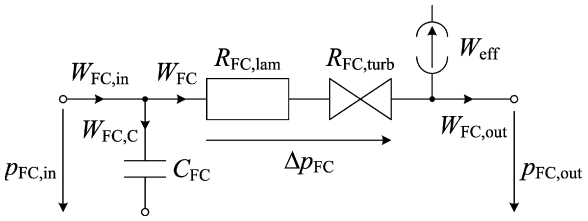

Fig. 3. Equivalent circuit of the fuel cell stack with effective mass flow W_{eff}.

The differential equation of the inlet with $K_{in,exp} = 2$ is

$$W_{in} = C_{in} \cdot \dot{p}_{in} + \frac{p_{in} - p_{FC,in}}{R_{in}} \tag{9}$$

with the flow resistance

$$R_{in} = \frac{1}{\sigma_{in}} \cdot (K_{in,lam} + K_{in,turb} \; W_{FC,in}). \tag{10}$$

The differential equation of the outlet with $K_{out,exp} = 2$ is

$$W_{out} = C_{out} \cdot \dot{p}_{FC,out} + \frac{p_{FC,out} - p_V}{R_{out}} \tag{11}$$

with the flow resistance

$$R_{out} = \frac{1}{\sigma_{out}} \cdot (K_{out,lam} + K_{out,turb} \; W_{out}). \tag{12}$$

For the valve which does not have the capability to store mass an algebraic equation

$$\sigma_V \cdot \Delta p_V = \sigma_V \cdot R_V \cdot W_{out} = K_{V,turb} W_{out}^{K_{V,exp}} \tag{13}$$

results with the flow resistance

$$R_V = \frac{1}{\sigma_V} \cdot K_{V,turb} \; W_{out}^{K_{V,exp}-1} \tag{14}$$

Equation (13) can be combined with the differential equation (11) to

$$W_{out} = C_{out} \cdot \dot{p}_{FC,out} + \frac{p_{FC,out} - p_{out}}{R_{Vout}} \tag{15}$$

with the sum of the flow resistances $R_{Vout} = R_V + R_{out}$.

The model of the fuel cell stack (Fig. 3) differs from the other submodels because of the electrochemical reaction that is taking place and the mass flows across the membrane which are modelled by an effective mass flow.

$$W_{FC} = W_{FC,eff} + W_{FC,out} \tag{16}$$

The differential equation of the fuel cell is

$$W_{FC,in} = C_{FC} \cdot \dot{p}_{FC,in} + \frac{p_{FC,in} - p_{FC,out}}{R_{FC}} \tag{17}$$

with the flow resistance

$$R_{FC} = \frac{1}{\sigma_{FC}} \cdot (K_{FC,lam} + K_{FC,turb} \; W_{FC}^{K_{FC,exp}-1}) \tag{18}$$

For the fuel cell stack, the model parameters may depend on the pressure level, the humidity and the current mass flow.

The structure of the model of the gas dynamics can be used both, for the anode and the cathode side of a fuel cell. The incorporated parameters were identified for both sides. In the following only the cathode side will be regarded.

2.2. Conversion of oxygen

The fuel cell reaction – at the cathode side the reduction of oxygen – couples the gas dynamics to the fuel cell current. The mass flow of the reacting oxygen

$$W_{react,O_2} = k_{react,O_2} \cdot I_{FC} \tag{19}$$

which contributes to the effective mass flow in the fuel cell is, with Faraday's law, proportional to the effective fuel cell current I_{FC}, where k_{react,O_2} is the proportionality constant.

The ratio of oxygen fed through the fuel cell W_{FC,O_2} to the oxygen consumed in the reaction W_{react,O_2}

$$\lambda_{O_2} = \frac{W_{FC,O_2}}{W_{react,O_2}} > 1 \tag{20}$$

is called excess ratio and is defined as the inverse of the conversion. Thereby, the mass flow of oxygen through the fuel cell is

$$\begin{aligned} W_{FC,O_2} &= y_{O_2} \cdot (W_{FC} - W_{FC,H_2O}) \\ &= y_{O_2} \cdot \left(\frac{p_{FC,in} - p_{FC,out}}{R_{FC}} - W_{FC,H_2O} \right) \end{aligned} \tag{21}$$

with the mass fraction of oxygen in air y_{O_2}.

For values of y_{O_2} close to one or less, not enough reactants flow through the fuel cell to sustain the reaction. In other words, starvation of fuel cells takes place, when less oxygen is fed to the cathode as is consumed in the reaction.

2.3. Models of the actuators

Besides the outlet valve, the mass flow controller and the electrical load are actuators of the fuel cell system. The dynamics of the mass flow controller (MFC) is modelled as a first-order lag element

$$W_d = \tau_{MFC} \cdot \dot{W}_{in} + W_{in} \tag{22}$$

with the desired mass flow W_d, the mass flow into the system W_{in}, and the time constant τ_{MFC} which describes the inertia of supplying an air mass flow into the system. If models of compressors or blowers exist they can be used instead.

The electrical load (EL) is also modelled as a first-order lag element

$$I_{EL,d} = \tau_{EL} \cdot \dot{I}_{FC} + I_{FC} \tag{23}$$

with the effective fuel cell current I_{FC}, the control signal of the electrical load $I_{EL,d}$, and a much smaller time constant τ_{EL}. By distinguishing between the control signal of the electrical load $\tau_{EL,d}$ and the desired load current I_d, the desired and the effective fuel cell current are decoupled. Thus, the current can be used as a control variable to avoid starvation. If the fuel cell is not connected directly to the load, dynamic models of the power electronics, e.g. inverters, can be used instead of equation (23).

2.4. State space description

2.4.1. Nonlinear continuous state space description

The gas dynamics together with the actuators form the controlled fuel cell system. The input or control variables of the system

$$\mathbf{u} = \begin{bmatrix} W_d & R_V & I_{FC,d} \end{bmatrix}^T \tag{24}$$

are directly linked to the mass flow controller, the outlet valve, and the electrical load as the actuators of the system. The state vector

$$\boldsymbol{x} = \begin{bmatrix} W_{in} & p_{in} & p_{FC,in} & p_{FC,out} & I_{FC} \end{bmatrix}^T \tag{25}$$

comprises the mass flow into the system, the pressure at the mass flow controller, the pressure at the inlet and the outlet of the fuel cell stack, and the effective fuel cell current. The output or controlled variables

$$\mathbf{y} = \begin{bmatrix} \lambda_{O_2} & p_{FC,in} & I_{FC} \end{bmatrix}^T \tag{26}$$

are the excess ratio of oxygen, the pressure at the inlet of the fuel cell and the fuel cell current.

Equations (22), (9), (17), (15) and (23) lead to a state space description

$$\dot{\mathbf{x}} = \mathbf{f}(\mathbf{x}, \mathbf{u}) = \tilde{\mathbf{A}}_c\,\mathbf{x} + \tilde{\mathbf{B}}_c\,\mathbf{u} + \mathcal{NL}_x(\mathbf{x}) + \mathcal{NL}_u(\mathbf{x})\,\mathbf{u} \tag{27}$$

with the constant system matrix $\tilde{\mathbf{A}}$, the input matrix $\tilde{\mathbf{B}}$, the vector of isolated nonlinearities $\mathcal{NL}_x(\mathbf{x})$, and the matrix of input affine nonlinearities $\mathcal{NL}_u(\mathbf{x})$. The output equation

$$\mathbf{y} = \mathcal{NL}_y(\mathbf{x}) \tag{28}$$

is also nonlinear.

2.4.2. Linearization

The vectors $\mathcal{NL}_x(\mathbf{x})$ and $\mathcal{NL}_u(\mathbf{x})$ are linearized by a first order linearization along the reference trajectory of the states, element by element. For example, an element $\mathcal{NL}_{x,i}(x_1, x_2)$ of the vector $\mathcal{NL}_u(\mathbf{x})$ that depends on the states x_1 and x_2 is approximated by

$$\begin{aligned}\mathcal{NL}_{x,i}(x_1, x_2) \approx\ & \mathcal{NL}_{x,i}(x_{1,\mathrm{ref}}, x_{2,\mathrm{ref}}) \\ & + \left.\frac{\mathrm{d}\mathcal{NL}_{x,i}}{\mathrm{d}x_1}\right|_{x=x_{\mathrm{ref}}} (x_1 - x_{1,\mathrm{ref}}) + \left.\frac{\mathrm{d}\mathcal{NL}_{x,i}}{\mathrm{d}x_2}\right|_{x=x_{\mathrm{ref}}} \\ & \times (x_2 - x_{2,\mathrm{ref}})\end{aligned} \tag{29}$$

The matrix $\mathcal{NL}_u(\mathbf{x})$ is linearized by a zeroth order linearization along the reference trajectory

$$\mathcal{NL}_u(\mathbf{x}) \approx \mathcal{NL}_u(\mathbf{x}_{ref}). \tag{30}$$

Therewith, the continuous state differential equation (27) can be rearranged to a linear state description

$$\dot{\mathbf{x}} = \mathbf{f}(\mathbf{x}, \mathbf{u}) \approx \mathbf{A}_c\,x + \mathbf{B}_c\,\mathbf{u} + \mathbf{v}_c \tag{31}$$

with the system matrix $\mathbf{A}_c$, the input matrix $\mathbf{B}_c$, and the offset vector $\mathbf{v}_c$. The linearized output equation results to

$$\mathbf{y} = \mathcal{NL}_y(\mathbf{x}) \approx \mathbf{C}\,\mathbf{x} + \mathbf{v}_y \tag{32}$$

with the output matrix $\mathbf{C}$, and the offset vector $\mathbf{v}_y$. Both offset vectors merely depend on the reference trajectory of the state vector.

2.4.3. Discretization

For the numerical calculation of the control variables the system needs to be discretized. Thereby it is assumed that the input $\mathbf{u}$ and the offset $\mathbf{v}_c$ are piecewise constant over a sampling period. Discretization yields a discrete state space description

$$\mathbf{x}_{k+1} = \mathbf{A}_d\,\mathbf{x}_k + \mathbf{B}_d\,\mathbf{u}_k + \mathbf{v}_d \tag{33}$$

with the system matrix $\mathbf{A}_d = e^{A_c T}$, the input matrix $\mathbf{B}_d = \int_0^T e^{-A_c \nu} \cdot \mathbf{B}_c\,\mathrm{d}\nu = (A_d - I) \cdot \mathbf{A}_c^{-1} \cdot \mathbf{B}_c$ and the offset vector $v_d = \int_0^T e^{-\boldsymbol{A}_c \nu} \cdot v_c\,\mathrm{d}\nu = (\boldsymbol{A}_d - \boldsymbol{I}) \cdot \boldsymbol{A}_c^{-1} \cdot v_c$. The output equation remains unchanged

$$\mathbf{y}_k = \mathbf{C}\,\mathbf{x}_k + \mathbf{v}_y \tag{34}$$

The index k indicates the discrete time index for the point in time $t_k = k{\cdot}T$, with the sampling time T.

3. Model predictive control

Model predictive control is a multivariable control that takes account of actuator limitations as well as state and output constraints. The predictive controller has an internal model which is used to predict the behaviour of the system depending on the input variables over a prediction horizon. Thereby, the prediction horizon H_p is the number of time increments for the forecast.

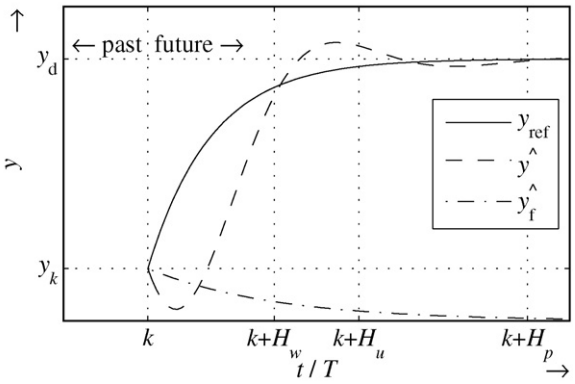

Fig. 4. MPC receding horizon, reference trajectory y_{ref}, desired and predicted output variable, y_d and $\hat{y}$.

Figs. 4 and 5 illustrate the idea of the receding horizon of a single-input and single-output (SISO) system. In Fig. 4 the measured output y_k at the time $t = k{\cdot}T$ shows a difference to its desired value y_d. To approach the desired value smoothly an exponential reference trajectory

$$y_{\mathrm{ref}} = y_d - (y_d - y_k) \cdot e^{-\frac{t}{\tau_{\mathrm{ref}}}} \tag{35}$$

with a defined time constant τ_{ref} is calculated for the output. The task of the optimal controller is to optimise the sequence of input changes in Fig. 5 so that the predicted output $\hat{y}$ over a prediction horizon of H_p time increments yields a minimum error to the reference trajectory. Thereby, the evaluation of the error can be limited to the time window $t \in [(H_w + k)T;\ (H_p + k)T]$ at the end of the prediction horizon and the input variable can be left unchanged after H_u time increments. If the optimal trajectory of the input variable is found, the first input change is applied to the system. For each time increment the prediction horizon is shifted and the input is calculated again.

For a linear model the solution is found analytically. If the solution does not fulfil the constraints the global minimum is found solving a quadratic programming problem by the active set method.

3.1. Prediction of the controlled variables

The system model in form of the linear discrete state space description in equations (33) and (34) enables a prediction of the output variables by computationally fast matrix–vector operations. The predicted output variables over the prediction horizon are in matrix–vector form [11,12].

$$\hat{\boldsymbol{Y}} = \boldsymbol{\Psi} \cdot \boldsymbol{x}_k + \boldsymbol{\Gamma} \cdot \boldsymbol{u}_{k-1} + \boldsymbol{G}_x \cdot v_d + \boldsymbol{G}_y \cdot v_y + \boldsymbol{\Theta} \cdot \Delta\hat{\boldsymbol{U}} = \hat{\boldsymbol{Y}}_f + \boldsymbol{\Theta} \cdot \Delta\hat{\boldsymbol{U}} \tag{36}$$

The vector of the predicted output variables $\hat{\boldsymbol{Y}}$ is a function of the current state vector $\mathbf{x}_k$, the preceding input vector $\mathbf{u}_{k-1}$, the offsets

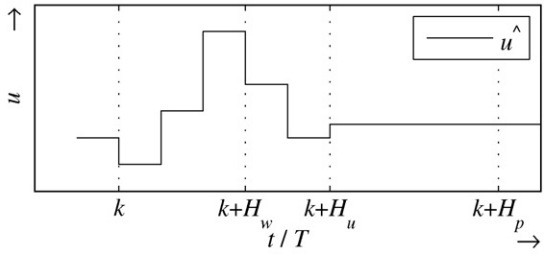

Fig. 5. MPC receding horizon, input variable u.

$\mathbf{v}_d$ and $\mathbf{v}_y$ and the future changes of the input vector $\Delta\hat{\boldsymbol{U}}$. The lengthy definition of the matrices $\boldsymbol{\Psi}$, $\boldsymbol{\Gamma}$, $\mathbf{G}_x$, $\mathbf{G}_y$ and $\boldsymbol{\Theta}$ is to be found in the cited references. The output is composed of the influence of future input changes $\boldsymbol{\Theta}\cdot\Delta\hat{\boldsymbol{U}}$ and the free response $\hat{\boldsymbol{Y}}_f$ which describes the output behaviour in the case the input would not be changed.

The following sources of error lead to an accumulated error in the predicted output:

- Errors in the continuous model
- Calculation of the reference trajectory
- Linearization along the reference trajectory
- Discretization
- Simplifying assumptions as piecewise constant offsets over a sampling period.

For the fuel cell system model the error of the predicted output is sufficiently small to calculate an optimal input trajectory as described in the following.

3.2. Unconstrained optimisation of the control variables

The optimum which is searched in the model predictive control scheme is characterised by a minimum error of the predicted output to the reference trajectory, and additionally a minimum of changes of the input variable to save actuating energy. The discrete objective function which has to be minimised is

$$J = \sum_{i=H_w}^{H_p} ||\hat{y}_{k+i} - y_{ref,k+i}||^2_{Q(i)} + \sum_{i=0}^{H_u-1} ||\Delta u_{k+i}||^2_{R(i)}$$

$$= ||\hat{\boldsymbol{Y}} - \boldsymbol{Y}_{ref}||^2_{\boldsymbol{Q}} + ||\Delta\hat{\boldsymbol{U}}||^2_{\boldsymbol{R}} \quad (37)$$

with the diagonal weighting matrices $\mathbf{Q}$ and $\mathbf{R}$. It can be expressed with sums and in matrix–vector form. As discussed above, the difference of the predicted output to the reference trajectory $\hat{y} - y_{ref}$ does not need to be penalized at all times over the prediction horizon. It is sufficient to penalize only the error at the last H_p–H_w time increments. On the other hand, the trajectory of the input values can be chosen constant after H_u steps. Therewith, less input moves need to be optimised.

Introducing the tracking error

$$\boldsymbol{E} = \boldsymbol{Y}_{ref} - \hat{\boldsymbol{Y}}_f = \boldsymbol{Y}_{ref} - (\boldsymbol{\Psi}\cdot\boldsymbol{x}_k + \boldsymbol{\Gamma}\cdot\boldsymbol{u}_{k-1} + \boldsymbol{G}_x\cdot v_d + \boldsymbol{G}_y\cdot v_y) \quad (38)$$

as the difference between the reference trajectory and the free response for no input changes the objective function can be rearranged [11]. To find the optimal input changes the gradient of the objective function is set to zero. The resulting vector of the optimal input changes can be calculated analytically

$$\Delta\hat{\boldsymbol{U}}_{opt} = 0.5\cdot(\boldsymbol{\Theta}^T\boldsymbol{Q}\,\boldsymbol{\Theta} + \boldsymbol{R})^{-1}\cdot 2\,\boldsymbol{\Theta}^T\boldsymbol{Q}\,\boldsymbol{E}. \quad (39)$$

To solve the optimisation numerically it is formulated as a least-squares problem with the square roots $\mathbf{S}_Q$ and $\mathbf{S}_R$ of the positive definite, diagonal weighting matrices $\mathbf{Q}$ and $\mathbf{R}$. $\Delta\hat{\boldsymbol{U}}_{opt}$ is the least-squares solution of the equation

$$\begin{bmatrix} \boldsymbol{S}_Q\,\boldsymbol{\Theta} \\ \boldsymbol{S}_R \end{bmatrix} \Delta\hat{\boldsymbol{U}} = \begin{bmatrix} \boldsymbol{S}_Q\,\boldsymbol{E} \\ \mathbf{0} \end{bmatrix} \quad (40)$$

which can be solved for $\Delta\hat{\boldsymbol{U}}_{opt}$ using, e.g. the *MATBLAB* matrix left division.

3.3. Constrained optimisation of the control variables

If the allowed range of the input and output variables is limited a constrained optimisation problem has to be solved. The optimisation problem of the MPC with inequality constraints has the form of a quadratic programming (QP) problem. There are standard algorithms available to solve QP problems subject to inequality constraints as for example the active set method [13,14], which is used in the *MATLAB*-function *linprog*. If no constraint are active the global optimum is found solving the least-squares problem in equation (40). If one or more constraints are active, the method finds the minimum feasible solution of the QP problem subject to the constraints.

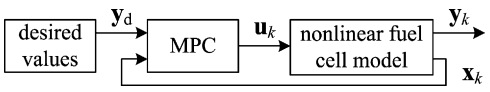

Fig. 6. Structure of the closed loop control circuit.

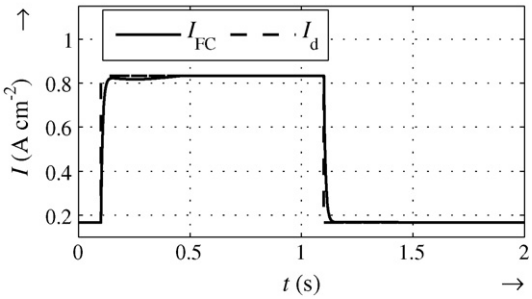

Fig. 7. Trajectory of the desired and the effective fuel cell current, I_d and I_{FC}.

4. Control design for the fuel cell system

Fig. 6 shows the structure of the control loop with the vector of the desired values $\mathbf{y}_d$, the model predictive controller (MPC) which embraces the prediction of the output and the optimisation of the input, and the nonlinear fuel cell model.

The vector of the desired values for the outputs is

$$\boldsymbol{y}_d = \begin{bmatrix} \lambda_d & p_{FC,d} & I_d \end{bmatrix}^T, \quad (41)$$

where $\lambda_d = 2$ and $p_{FC,d} = 1.5$ bar are constant set points and $I_d = I_d(t)$ is the trajectory of the desired load current.

The actuators of the fuel cell system are subject to limitations which may be due to physical limits or due to the balance of plant. On the one hand the flow resistance of the valve is physically limited to a minimum value determined by its cross sectional area and the mass flow controller is only able to supply a maximum mass flow into the system. On the other hand, the desired mass flow is arbitrarily limited to a minimum value to sustain the reaction and to humidify the membrane. These actuator limitations result in an inequality equation for the input variables: $\mathbf{u}_{min} \le \mathbf{u}_k \le \mathbf{u}_{max}$.

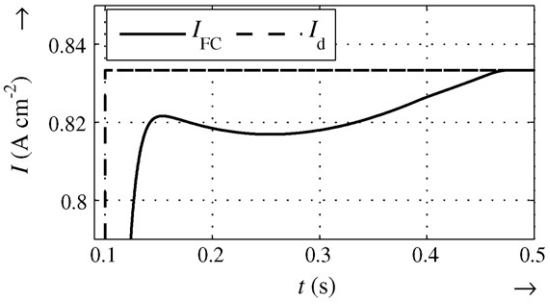

Fig. 8. Detail of the trajectory of the desired and the effective fuel cell current of Fig. 7.

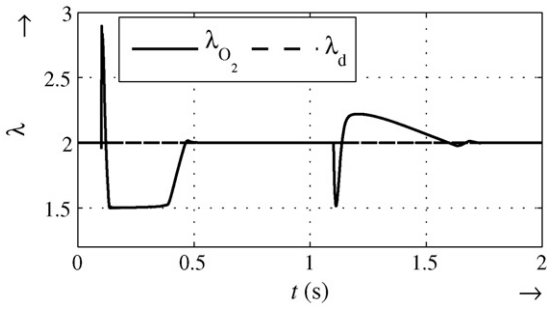

Fig. 9. Trajectory of the constraint excess ratio $\lambda_{O_2} > 1$.

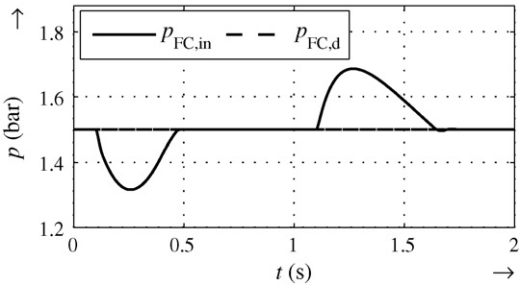

Fig. 10. Trajectory of the cathode pressure $p_{FC,in}$.

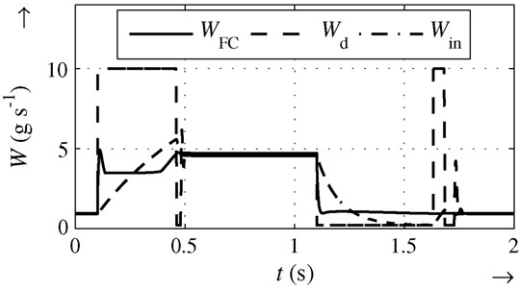

Fig. 11. Trajectory of the mass flow through the fuel cell stack W_{FC}, the desired, limited mass flow at the MFC W_d, and the mass flow into the system W_{in}.

Since the target of the control design is to allow dynamic load changes without damaging the fuel cell, the output variables need to be constrained: $\mathbf{y}_{min} \leq \mathbf{y}_k \leq \mathbf{y}_{max}$. Especially to avoid starvation the fuel cell pressure and the excess ratio of oxygen must not fall beyond a minimum value. Hence, the excess ratio of oxygen is limited to a minimum value of $\lambda_{min} = 1.5$ and the fuel cell pressure to a value of $p_{min} = 0.5$ bar.

The control design and the simulation of the nonlinear model is realised in *MATLAB*/*Simulink* using embedded *MATLAB* files in *Simulink*. Thereby, the sampling time of the prediction is set to $T = 1$ ms and the prediction horizon to 10 ms. The reference trajectories of the output variables are generated according to equation (35) with the time constants $\tau_\lambda = 10$ ms, $\tau_p = 10$ ms and $\tau_I = 5$ ms for the excess ratio, the pressure, and the current. As reference trajectory for the state variables the prediction of the preceding point of time t_{k-1} are used.

5. Results

To the controlled fuel cell system a rectangular load profile as depicted in Fig. 7 is applied.

Figs. 7–11 show the response of the closed loop to the load profile. As can be seen in Fig. 7 and in detail in Fig. 8 the MPC reduces the slope of the effective fuel cell current in comparison to the desired current due to the exponential reference trajectory and reduces the current itself, when constraints are active as in Fig. 9 the excess ratio. The fuel cell current is not increased again until the constraint of the excess ratio gets inactive. Subsequent, the effective fuel cell current reaches its desired value without overshooting.

Fig. 10 shows that at the rising fuel cell current the pressure at the fuel cell drops, but without approaching the constraint. At the falling fuel cell current for a short period of time the pressure is higher than the desired value.

Fig. 11 shows the active actuator limitations. At the fast load change towards higher currents the desired mass flow reaches its maximum value and keeps it until the excess ratio and the pressure reach their desired values.

The MPC successfully performs the task of guaranteeing a minimum value of the excess ratio and thereby enables a dynamic fuel cell operation.

6. Conclusion

The presented model of the fuel cell system which incorporates the gas dynamics, the coupling of the fuel cell current to the mass flow, and the models of the actuators is used in a linearized and discretized form as the internal model of a predictive control scheme. The presented control design prevents fuel cell starvation by guaranteeing a minimum value of the excess ratio of oxygen and a minimum value of the fuel cell pressure. The controller additionally integrates actuator limitations in its calculation of the optimal control inputs. As the results show, the application of model predictive control to the nonlinear model of the fuel cell system increases the dynamics, the reliability and the durability of the fuel cell.

The presented results of the designed controller demonstrate the applicability of model predictive control approaches to nonlinear fuel cell models. To reduce the computational costs of the optimisation the implemented algorithm has to be transferred into C-code. If further reductions are needed alternative model predictive control schemes can be applied [15,16].

References

[1] W. Schmittinger, A. Vahidi, J. Power Sources 180 (2008) 1–14.
[2] J.P. Meyers, R.M. Darling, J. Electrochem. Soc. 153 (2006) A1432–A1442.
[3] A.A. Franco, M. Gerard, J. Electrochem. Soc. 155 (2008) B367–B384.
[4] A. Vahidi, A. Stefanopoulou, H. Peng, Proc. Am. Control Conf., Boston, MA, 2004, pp. 834–839.
[5] J. Golbert, D.R. Lewin, Proc. 16th IFAC World Congress, Prague, 2005.
[6] J. Sun, I. Kolmanovsky, Proc. American Control Conference, Boston, MA, 2004, pp. 828–833.
[7] H. Töpfer, P. Besch, Grundlagen der Automatisierungstechnik (in German), Carl Hanser Verlag, 1990.
[8] G. Schmidt, Grundlagen der Regelungstechnik (in German), Springer, 1991.
[9] M.A. Danzer, J. Wilhelm, H. Aschemann, E.P. Hofer, J. Power Sources 176 (2008) 515–522.
[10] M.A. Danzer, G. Schlumberger, M. Wörz, E.P. Hofer, Modelling, 5th Symposium on Fuel Cell Modelling and Experimental Validation, Winterthur, Switzerland, 2008.
[11] J. Maciejowski, Predictive Control with Constraints, Prentice Hall, 2002.
[12] M. Rau, Nichtlineare modellbasierte prädiktive Regelung auf Basis lernfähiger Zustandsraummodelle (in German), Ph.D. Thesis, TU München, 2003.
[13] J. Nocedal, S.J. Wright, Numerical Optimization, Springer, 2006.
[14] R. Fletcher, Practical Methods of Optimization, John Wiley & Sons, 2006.
[15] F. Lizarralde, J.T. Wen, L. Hsu, Proc. American Control Conference, San Diego, California, 1999, pp. 4263–4267.
[16] S. Jung, J.T. Wen, ASME J. Dyn Syst., Measure. Control 126 (2004) 666–673.